Iron-Plasma Transmission Measurements at Temperatures Above 150 eV

J. E. Bailey,[1] G. A. Rochau,[1] C. A. Iglesias,[2] J. Abdallah, Jr.,[3] J. J. MacFarlane,[4] I. Golovkin,[4] P. Wang,[4] R. C. Mancini,[5]
P. W. Lake,[1] T. C. Moore,[6] M. Bump,[6] O. Garcia,[6] and S. Mazevet[7]

[1]*Sandia National Laboratories, Albuquerque, New Mexico 87185, USA*
[2]*Lawrence Livermore National Laboratory, University of California, Livermore, California 94550, USA*
[3]*Theoretical Division, Los Alamos National Laboratory, Los Alamos, New Mexico 87545, USA*
[4]*Prism Computational Sciences, Madison, Wisconsin, USA*
[5]*University of Nevada, Reno, Nevada, USA*
[6]*K-tech Corporation, Albuquerque, New Mexico, USA*
[7]*Department de Physique Theorique et Appliquee, CEA, Bruyeres Le Chatel, France, BP12 91680*

Measurements of iron-plasma transmission at 156 ± 6 eV electron temperature and $6.9 \pm 1.7 \times 10^{21}$ cm^{-3} electron density are reported over the 800–1800 eV photon energy range. The temperature is more than twice that in prior experiments, permitting the first direct experimental tests of absorption features critical for understanding solar interior radiation transport. Detailed line-by-line opacity models are in excellent agreement with the data.

PACS numbers: 52.25.Os, 52.58.Lq, 52.72.+v, 95.30.Ky

Radiation transport in high energy density plasmas, including inertial confinement fusion (ICF), z pinch radiation sources, and stellar interiors, depends on the opacity. The myriad bound-bound (b-b) and bound-free (b-f) transitions associated with heavier elements require an approximate treatment of the opacity and experimental tests are vital. Progress has been hindered by the lack of experiments at temperatures above 70 eV. For example, the present discrepancy between solar models and helioseismology could be resolved by an $\sim 20\%$ increase in the mean opacity. Determining whether this discrepancy originates in opacity model deficiencies or in some other aspect of the solar model would be an important step toward better understanding of the sun [1].

Most opacity experiments use x rays to uniformly heat a sample and measure the spectrally resolved transmission with a spectrometer that views a backlighter through the sample. Measurements become more challenging at high temperature because the heat source must supply more energy and the backlight source must be brighter to overwhelm the sample self-emission. In this Letter we report on Fe transmission measurements at electron temperature $T_e = 156$ eV and electron density $n_e = 6.9 \times 10^{21}$ cm^{-3} over the photon energy range $h\nu \sim 800$–1800 eV. The temperature is more than $2\times$ higher than in prior work, permitting the first tests of opacity models for b-b transitions important in solar interior radiation transport [1]. Similar transitions in Cu influence Cu-doped Be ICF capsule implosions [2].

Our goal is to test physical issues and approximations used in opacity models, since it is impractical to perform experiments over all relevant conditions. A few of the many issues are b-b transition bundling into unresolved arrays, inclusion of multiply excited states and low probability transitions, and spectral line broadening. Which issues can be addressed depends on the plasma conditions

and the measured spectral range. The former must produce the relevant charge states and the latter must include the relevant b-b and b-f transitions. For example, consider iron-plasma opacity calculated [3] at $T_e = 182$ eV and $n_e = 9 \times 10^{22}$ cm^{-3}, conditions [4] corresponding to the solar radiation-convection boundary (Fig. 1). Iron is important in stars because it is relatively abundant and the huge number of b-b and b-f transitions provides large absorption. The plasma consists mainly of ions with 0, 1, or 2 vacancies in the L shell. L shell b-b transitions dominate the absorption for $h\nu \sim 700$–1500 eV, while b-f and b-b M shell transitions with excited initial states dominate at lower photon energies. The present experiment T_e and n_e values are $1.2\times$ and $10\times$ lower than at the solar radiation-convection boundary, respectively. Nevertheless, these conditions produce similar charge states and the transitions dominating the opacity are similar (Fig. 1). Therefore, these experiments investigate absorption by the partially-filled L shell iron ion configurations predominant in much of the solar interior. Tests of other issues such as line broadening in the solar interior await further experimental advances.
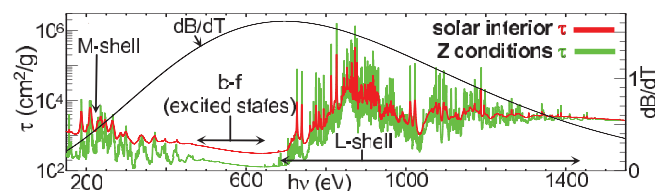
FIG. 1 (color). Iron opacity calculated at the radiation-convection boundary in the sun (red) and at the conditions in Z experiments (green). The Planck function derivative with respect to temperature evaluated at 182 eV (black) illustrates the photon energies most important for the solar radiation transport.

Prior work [5,6] established experimental requirements that include uniform plasma, independent T_e and n_e diagnosis, accounting for self-emission, and accurate transmission measurements. L shell absorption in partially open M shell ions was measured [5–7] over $h\nu \sim 700$–2000 eV in plasmas with $T_e \sim 20$–60 eV. However, the measurements did not address the 10–240 eV photon energy range that dominates the transport at these temperatures. Subsequent experiments [8] probed 80–300 eV photon energies and provided new insight into stellar envelopes, but the low temperatures precluded opacity model tests needed for stellar interiors, ICF capsules, and z pinches.

The challenges of higher temperature opacity experiments were overcome here using the dynamic hohlraum x-ray source [9] at the Sandia National Laboratories Z facility. The process entails accelerating an annular tungsten z-pinch plasma radially inward onto a cylindrical low density CH_2 foam (Fig. 2), launching a radiating shock that propagates toward the cylinder axis. Radiation trapped by the tungsten plasma forms a hohlraum. A sample attached to the top diagnostic aperture is heated during the ~ 9 ns period when the shock is propagating inward (Fig. 2) and the radiation temperature rises above 200 eV. When the shock reaches the axis, the brightness temperature in an ~ 0.5 mm diameter spot was measured using a combination of x-ray diodes and gated pinhole cameras to exceed 300 eV for ~ 1–3 nsec. This provides an extremely bright backlight source that spans a broad photon energy range. The almost featureless spectrum promotes accurate transmission measurements [10].

The samples consisted of an Fe/Mg mixture fully-tamped [6] on both sides by 10-μm-thick parylene-N (CH). The CH thickness is approximately 10$\times$ larger than in prior experiments, contributing to the plasma uniformity [11]. The Fe/Mg mixture was fabricated by depositing 10 alternating Mg and Fe layers. *In situ* methods were used to infer the areal density ρx. This demands self-consistency in model calculations of the b-f and b-b absorption and is only possible because of the broad photon energy range. The Mg ρx was determined by compar-

ing the He-like absorption line strengths with PRISMSPECT [3] calculations. He-like is the most abundant Mg ion stage, with less than 1% abundance change over the T_e and n_e error bars determined below. The Fe ρx was determined by comparing the b-f continuum transmission with PRISMSPECT calculations in the 1380–1550 eV photon energy range that is relatively free of contributions from Fe b-b transitions. The Fe ρx uncertainty is dominated by the transmission and charge state distribution uncertainties. The Fe L shell b-f cross section is believed known to within a few percent [12] and continuum self-emission is negligible. The transmission uncertainty leads to approximately $\pm 25\%$ ρx uncertainty, and the Fe population variation over the T_e and n_e error bars contributes another $\pm 10\%$. Experiments were conducted in two groups using either a thicker Fe sample or a thinner Fe sample. The Mg areal density was 3.1×10^{-5} g/cm^2 in both groups. The Fe areal density was 6.1×10^{-5} g/cm^2 and 3.2×10^{-5} g/cm^2 in the thick-Fe and thin-Fe experiments, respectively.

Spectra were measured using a pair of convex potassium-acid-phthalate crystal spectrometers oriented at 9 deg with respect to the z-pinch axis (Fig. 2) and a 3.5 m source-to-crystal distance. Each spectrometer measures two space-resolved spectra using a pair of slits ranging from 100–600 μm wide (magnification = 1.0) and up to four spectra are recorded on Kodak 2492 film in each experiment. The spectral resolution measured at 1012 eV and 1486 eV was $E/\delta E \sim 700$. A typical absorption spectrum is shown in Fig. 2. Lineouts are taken through the central 400 μm region, corrected for the dispersion [13,14] and film response [15], the background is subtracted, and the transmission is determined by dividing the signal from experiments with and without the Fe/Mg. The absolute transmission varies by approximately $\pm 11\%$, primarily due to backlight brightness and spectrometer sensitivity changes. The accuracy was improved by averaging the transmission from the 12 thick-Fe measurements and the four thin-Fe measurements (Fig. 3). The averaging procedure exploited an opacity window at $h\nu \sim 1035$ eV
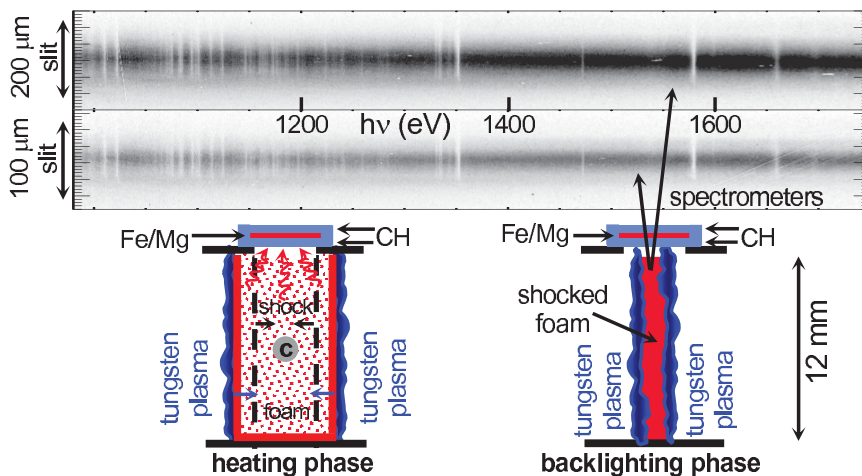
FIG. 2 (color). Schematic experiment diagram. Space-resolved spectra from one of the thick sample experiments are shown above the diagrams.
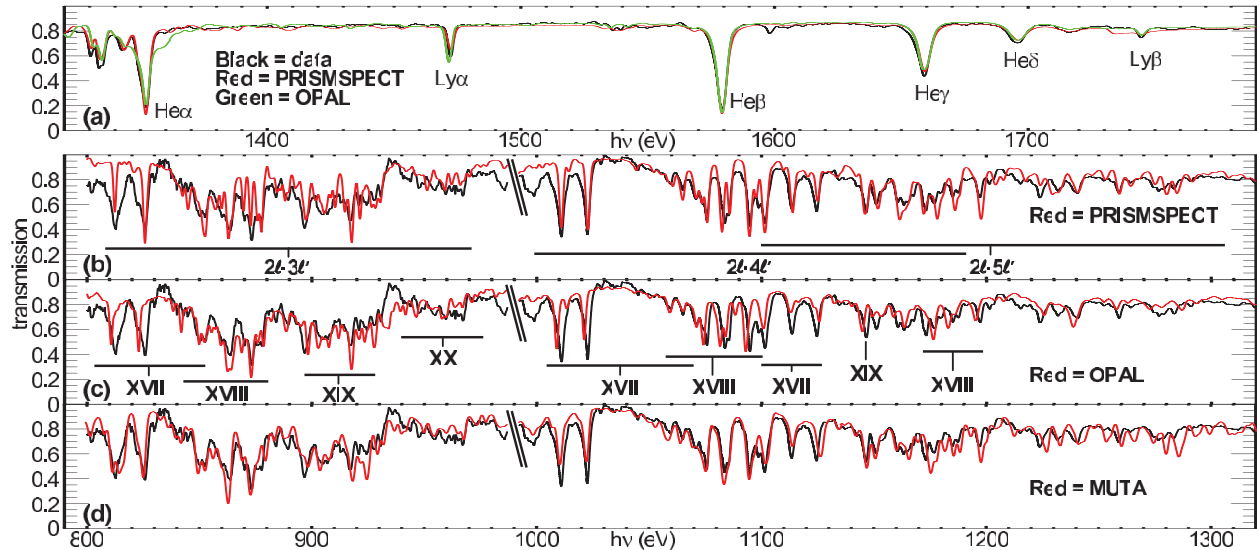
FIG. 3 (color).   Average experimental transmission from the thick samples (black line, $h\nu > 990$ eV) and the thin samples (black line, $h\nu < 990$ eV). The spectral range including the Fe b-f and Mg K shell (a) is compared with PRISMSPECT (red) and OPAL (green). Comparisons in the Fe L shell spectral energy range are shown for PRISMSPECT (b), OPAL (c), and MUTA (d) (models in red). The charge states and configurations responsible for many of the strong absorption features are indicated, although millions of b-b transitions are present.

with mean transmission $T = 0.96 \pm 0.04$ (thick-Fe data). The unattenuated backlight intensity was adjusted to force the transmission to equal this mean value at $h\nu \sim 1035$ eV in each experiment prior to averaging. The uncertainty in the mean transmission is a convolution of the approximately $\pm 4\%$ uncertainty in the $h\nu \sim 1035$ eV transmission with the relative transmission uncertainty as a function of photon energy. The relative uncertainties were $\pm 2\%$ and $\pm 5\%$ averaged over $h\nu \sim 990$–1305 eV and $h\nu \sim 800$–990 eV, respectively. The transmission in Fig. 3 corresponds to the thick-Fe group in the 990–1770 eV range and to the thin-Fe group in the 800–990 eV range. The larger number of measurements renders the thick-Fe data more accurate, but experimental problems prevented 800–990 eV data acquisition in this group. Using an average transmission from a number of measurements greatly improves signal-to-noise, an approach that is possible due to experiment reproducibility and, to the best of our knowledge, is unprecedented in opacity research.

The transmission scales with sample thickness according to $T_1 = T_2^{x1/x2}$, where T_1 and T_2 are transmissions of samples with thickness x_1 and x_2, respectively. The scaled thin-Fe transmission agrees with the thick-Fe transmission (Fig. 4), providing strong evidence that experimental errors due to self-emission, gradients, and background subtraction are small [16]. The self-emission was also determined to be negligible by comparing the calculated self-emission for a 155 eV plasma with the measured backlight brightness. Furthermore, the space-resolved measurements enabled observations of the plasma region that was heated but not backlit. No self-emission was detected.

The Mg absorption features were used to characterize the plasma. The density determined by comparing the Mg

He β, γ, and δ lines with calculated Stark-broadened profiles [17] was $n_e = 6.9 \times 10^{21}$ cm^{-3} $\pm 25\%$. The relative strengths of the Mg lines were used to infer [3] $T_e = 156$ eV $\pm 4\%$, assuming Local Thermodynamic Equilibrium (LTE). The uncertainties include contributions from measurement errors, shot-to-shot variations, and the influence of density variations on the inferred T_e, but do not include model uncertainties. The LTE approximation is reasonable because the Mg line opacities and the external radiation source both help drive the populations toward LTE. The impact of possible deviations from LTE was estimated to be small (compared to the uncertainties above) using non-LTE PRISMSPECT calculations that incorporate our current understanding of the radiation field at the sample. Matching the spectrum with calculations at a single T_e and n_e value implies that the effect of plasma nonuniformities is small.

The measurements were compared with the PRISMSPECT [3], OPAL [18], and MUTA [19] opacity models (Fig. 3). PRISMSPECT and OPAL use Detailed Term Accounting to compute the Fe XVI–XX b-b transitions, but the calculation of ionization balance and plasma effects rely on different methods. The OPAL calculations use an innova-
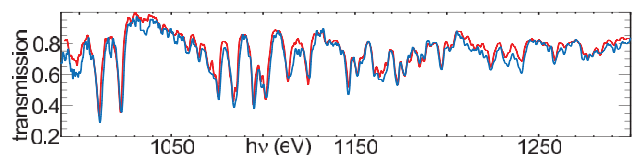
FIG. 4 (color).   Thick sample experiment mean transmission (red) compared with the thin sample experiment scaled mean transmission ($T_{scaled} = T_{thin}^{1.9}$, blue).

tive determination of the ionization balance and include explicit calculation for more than 100×10^6 Fe L shell spectral lines. The PRISMSPECT calculations include fewer explicitly calculated Fe L shell lines ($\sim$1 million), but use available data [13] to improve the wavelength and transition probability accuracy. MUTA uses a combination of Detailed Term Accounting and the Unresolved Transition Array approaches. The PRISMSPECT and OPAL calculations treated a mixed Fe/Mg plasma self-consistently while the MUTA calculation considered a pure Fe plasma with the ion density adjusted to provide the correct electron density. The genesis and approach followed in the three models is substantially different.

The Fig. 3 comparisons assume LTE at the plasma conditions determined from the Mg spectrum. This approximation was supported by Fe spectral calculations using the non-LTE version of the PRISMSPECT code and by the fact that both the Fe and Mg spectra are matched by independent LTE models at a single temperature and density. The T_e and n_e values were varied within the 1σ uncertainty limits and best agreement with the Fe b-b transitions was found at $T_e = 150$ eV and $n_e = 8.6 \times 10^{21}$ cm^{-3}. These conditions produce an average Fe ionization of 16.91, 16.58, and 16.13 from the PRISMSPECT, OPAL, and MUTA models, respectively.

The comparisons (Fig. 3) demonstrate that all three models are in excellent agreement with the Fe transmission data. The average difference between the models and data was approximately 8.0% in the 1005–1320 eV range and 10–16% in the 800–1005 eV range. These modern detailed opacity models provide impressive accuracy for L shell transitions in atoms with L shell vacancies. Nevertheless, statistically significant deviations between the models and the data exist for specific spectral features. The reduced χ^2 is approximately unity over some portions of the spectrum, indicating excellent agreement [20]. However, in other regions (e.g., the Ne-like Fe $2p$-$3d$ and $2p$-$4d$ features), $\chi^2 > 10$. These discrepancies could arise from residual systematic experiment errors, model deficiencies, or both.

The implications of these results for the physics treatments embedded in each opacity model are beyond the scope of this Letter. Also, the results do not necessarily imply that calculations performed for applications (e.g., the solar interior) possess the same accuracy. An extensive detailed level description that accounts for myriad spectral lines was used to obtain the agreement shown here. Applications may require models employing different approximations, a more limited level description, or statistical averaging, and the work described here provides a new ability to estimate the accuracy compromises that result.

We thank the Z dynamic hohlraum, accelerator, diagnostics, materials processing, target fabrication, and wire array teams for invaluable and dedicated technical assistance. Special assistance was provided by L. Nielsen-

[1] J. N. Bahcall, A. M. Serenelli, and M. Pinsonneault, Astrophys. J. **614**, 464 (2004); S. Basu and H. M. Antia, Astrophys. J. **606**, L85 (2004); H. M. Antia and S. Basu, Astrophys. J. **620**, L129 (2005); J. N. Bahcall, A. M. Serenelli, and S. Basu, Astrophys. J. **621**, L85 (2005).
[2] S. Hann *et al.*, Phys. Plasmas **12**, 056316 (2005).
[3] J. J. MacFarlane *et al.*, High Energy Density Phys. **3**, 181 (2007).
[4] J. N. Bahcall *et al.*, Rev. Mod. Phys. **54**, 767 (1982).
[5] S. J. Davidson *et al.*, Appl. Phys. Lett. **52**, 847 (1988); T. S. Perry *et al.*, Phys. Rev. Lett. **67**, 3784 (1991); J. M. Foster *et al.*, *ibid.* **67**, 3255 (1991).
[6] T. S. Perry *et al.*, Phys. Rev. E **54**, 5617 (1996).
[7] C. Chenais-Popovics *et al.*, Astrophys. J. Suppl. Ser. **127**, 275 (2000); C. Chenais Popovics *et al.*, Phys. Rev. E **65**, 016413 (2001); J. E. Bailey *et al.*, J. Quant. Spectrosc. Radiat. Transfer **81**, 31 (2003); P. Renaudin *et al.*, *ibid.* **99**, 511 (2006).
[8] L. Da Silva *et al.*, Phys. Rev. Lett. **69**, 438 (1992); P. T. Springer *et al.*, *ibid.* **69**, 3735 (1992); G. Winhart *et al.*, J. Quant. Spectrosc. Radiat. Transfer **54**, 437 (1995); P. T. Springer *et al.*, *ibid.* **58**, 927 (1997).
[9] J. E. Bailey *et al.*, Phys. Plasmas **13**, 056301 (2006); T. W. L. Sanford *et al.*, Phys. Plasmas **13**, 012701 (2006).
[10] C. A. Iglesias, J. Quant. Spectrosc. Radiat. Transfer **99**, 295 (2006).
[11] C. A. Back *et al. ibid.* **58**, 415 (1997).
[12] G. V. Brown *et al.*, Phys. Rev. Lett. **96**, 253201 (2006); H. Chen *et al.*, Astrophys. J. **646**, 653 (2006).
[13] NIST Atomic Spectra Database (Version 3.1.2), http://physics.nist.gov/asd3.
[14] G. V. Brown, Astrophys. J. **502**, 1015 (1998); G. V. Brown *et al.*, Astrophys. J. Suppl. Ser. **140**, 589 (2002).
[15] B. L. Henke *et al.*, J. Opt. Soc. Am. B **1**, 828 (1984).
[16] T. S. Perry *et al.*, J. Quant. Spectrosc. Radiat. Transfer **54**, 317 (1995); D. J. Hoarty *et al.*, *ibid.* **99**, 283 (2006).
[17] L. A. Woltz and C. F. Hooper, Jr., Phys. Rev. A **38**, 4766 (1988); R. C. Mancini *et al.*, Comput. Phys. Commun. **63**, 314 (1991).
[18] C. A. Iglesias and F. J. Rogers, Astrophys. J. **464**, 943 (1996).
[19] S. Mazevet and J. Abdallah Jr., J. Phys. B **39**, 3419 (2006).
[20] P. R. Bevington and D. K. Robinson, *Data Reduction and Error Analysis for the Physical Sciences* (McGraw-Hill, New York, 1992).